

**VIETNAM ACADEMY OF SCIENCE AND TECHNOLOGY
INSTITUTE OF PHYSICS**

**The 8th Academic Conference on Natural Science
for Young Scientists Master & PhD. Students
from ASEAN Countries**

Vinh City, Vietnam. August 27-30, 2023



8th ASEAN

The 8th Academic Conference on **Natural Science**
for Young Scientists, Master & PhD Students
from ASEAN Countries

August 27-30, 2023

Vinh University, Vinh city, Nghe An province, Viet Nam

PROCEEDINGS



Publishing House for Science and Technology

VIETNAM ACADEMY OF SCIENCE AND TECHNOLOGY

INSTITUTE OF PHYSICS

**THE 8th ACADEMIC CONFERENCE ON
NATURAL SCIENCE FOR YOUNG SCIENTISTS,
MASTER AND PhD STUDENTS
FROM ASEAN COUNTRIES
(CASEAN - 8)**

Vinh City, Vietnam. 27-30 August 2023

PROCEEDINGS

ISBN: 978- 604- 357- 225-4

Publishing House for Science and Technology - 2023

COMPARISON OF EFFECTIVE REFRACTIVE INDEX AND DISPERSION CHARACTERISTICS OF CIRCULAR, HEXAGONAL LATTICES PCF WITH As₂S₃ SUBSTRATES

Trong Dang Van¹, Ngoan Le Thi¹, Duy Pham Dinh¹, Thuy Do Thanh¹, Vu Tran Quoc²,
Thuy Nguyen Thi⁴, Luong Thi Tu Oanh³, Lanh Chu Van^{1*}

¹*Department of Physics, Vinh University, 182 Le Duan, Vinh City, Vietnam*

²*Thu Khoa Nghia High School for The Gifted, Chau Doc City, Vietnam*

³*Nghe An College of Education, Vinh City, Viet Nam*

⁴*Hue University of Education, Hue University,
34 Le Loi Street, Hue City, Vietnam*

*E-mail: *chuvanlanh@vinhuni.edu.vn*

Abstract. This work performs a comparative study on two solid-core photonic crystal fibers (PCFs) with an As₂S₃ substrate. These two new photonic crystal fibers are designed using Lumerical Mode Solution software based on the finite element method. The introduced structure is a novel structure of six air-hole rings arranged in circular and hexagonal lattices. We analyze and compare the two structures' effective refractive index and dispersion characteristics with the change of filling factor (d/A). The PCF structures obtained dispersion characteristics diverse including all-normal dispersion and anomalous dispersion with one or two zero-dispersion wavelengths (ZDWs). Flat dispersion and closeness to the zero-dispersion curve in the long wavelength range are the advantages of these structures. The hexagonal lattice PCF structure possesses flat dispersion and is closer to the zero-dispersion curve than the structure with the circular lattice. Meanwhile, the real part of the effective refractive index of the circular lattice is always larger than the hexagonal lattice in the investigated wavelength range, and the effective refractive index decreases as the wavelength increases. Based on analysis and comparison, we have proposed structures with optimal dispersion and pump wavelength suitable for supercontinuum generation with a wide, flat, and smooth spectrum.

Keywords: *Photonic Crystal Fibers, Dispersion, Effective refractive index.*

I. INTRODUCTION

In 1996, at the Optical Fiber Conference (OFC) [1], Russell and colleagues announced a new type of optical fiber, the photonic crystal fiber (PCF). PCF is an optical fiber that uses photonic crystals to create a cladding around the core of the fiber. A photonic crystal is a medium formed from cyclically arranged micrometer-sized air holes that run along the entire length of an optical fiber, and this medium has a cyclically variable dielectric constant and a low loss [2].

Since then, PCF has attracted a great deal of interest from scientists around the world and has brought about a great development in optical fiber technology. In contrast to conventional optical fiber, PCF has more freedom in design and fabrication including guiding mechanism, size and shape of air hole, lattice constant and lattice type, etc. Geometric parameters along with the right material selection allow to control dispersion, transmission, and even nonlinear properties of the fiber. Today, PCF has been intensively studied and has many wide applications

in fiber lasers, optical amplifiers, nonlinear devices, high-power transmission lines, and highly sensitive gas sensors [3] and especially the application of supercontinuum generation (SCG) [4-7].

On the other hand, the large variation in the size and spacing of the air-hole (lattice constant) in the crust leads to a change in the optical properties of the PCF. The effective refractive index and dispersion of PCFs, which play an important role in the transmission mechanism of PCFs, can be controlled by adjusting the air-hole diameters (d) and lattice constants (Λ) of their air-hole arrays in the cladding. The difference in effective refractive index between the core and the crust not only determines the light confinement mechanism but also affects the confinement loss value, which is an important factor in improving the efficiency of SCG, which determines the spectral broadening performance of PCF. Therefore, optimizing the effective refractive index and dispersion characteristics is always targeted by researchers.

Until now, there have been many research works on PCF, usually focusing on three main types of PCF lattice including circular lattice [8, 9], square lattice [10, 11], and hexagonal lattice [12]. The outstanding results obtained from the above studies include high negative dispersion, low confinement loss, extremely large bandwidth, etc... These works have studied the influence of filling factor and lattice constant on the characteristics of PCF for each lattice structure, but have not simultaneously optimized the characteristics of PCF for each type of lattices. Most of the research works on solid core PCF with silica substrates have been studied extensively [13, 14, 15] because Silica has the advantages of purity, high chemical resistance, and high transparency from ultraviolet to infrared spectral range,... However, the limitation of Silica is its low nonlinear refractive index and its wavelength limit does not exceed 2 micrometers, resulting in low SCG efficiency. Meanwhile, Chalcogenide glass is said to be attractive because it has a nonlinearity 500 times higher than that of conventional silica [16] and the properties of PCF are obtained in the long wavelength range. Some work on Chalcogenide glass substances such as As_2Se_3 [17], and As_2S_3 [18-22] give good results.

In this paper, we design two new structures of circular lattice photonic crystal fibers and hexagonal lattice with six air-hole rings. We analyzed in detail the effective refractive index and dispersion characteristics of PCF with As_2S_3 substrates with the change of lattice constant and filling factor d/Λ . This substrate has a very high nonlinear refractive index ($n_{As_2S_3} = 420 \times 10^{-20} m^2/W$ [23]). In addition, we compared the effective refractive index and dispersion characteristics of PCF with 2 different types of structures and optimized to find structures with flat dispersion, close to zero dispersion in the long wavelength range suitable for SCG.

II. NUMERICAL MODELING

The geometric structure diagram of As_2S_3 substrate solid-core PCFs in the case of six rings modeled with different lattice types (cross-section) is shown in Fig. 1. As_2S_3 was chosen as the substrate material to create a difference in refractive index between the core and the crust to better limit the light in the core. Different from previous studies that designed 8 lattice rings, for this paper we design a PCF structure with 6 ordered lattice rings with the change of lattice constant (Λ). and fill factor (d/Λ). Where d is the diameter of the air holes and Λ is the distance

between the centers of two adjacent air holes. We use a lattice constant of 1.0 μm with the filling factor varying from 0.3 to 0.8 with a step of 0.05. The large core diameter is determined by the formula $D_c = 6\Lambda - d$. Lumerical Mode Solution software [24] based on the finite element method (FEM) was used for the simulations.

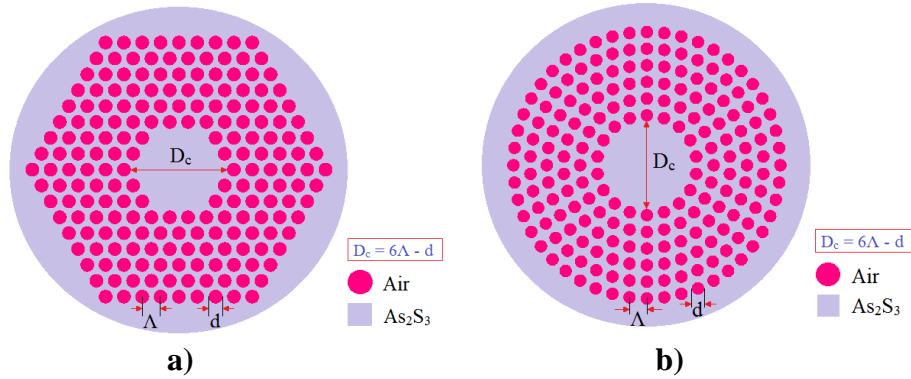


Fig. 1. Geometric structure of PCF with As_2S_3 substrate in case of six rings for two types of lattice: a) hexagonal lattice; b) circular lattice.

The nonlinear refractive index of As_2S_3 was obtained using the Sellmeier equation (1) [25] with the corresponding coefficients shown in Table 1.

$$n^2(\lambda) = 1 + \frac{A_1\lambda^2}{\lambda^2 - B_1} + \frac{A_2\lambda^2}{\lambda^2 - B_2} + \frac{A_3\lambda^2}{\lambda^2 - B_3} \quad (1)$$

The values of the conformance factors $A_1 \dots A_3$, and $B_1 \dots B_3$ are listed in Table 1 and λ are the wavelength of light in μm .

Table 1. The Sellmeier's coefficients of the As_2S_3 substrates.

Sellmeier's coefficients

Material	A_1	A_2	A_3	B_1 [μm^2]	B_2 [μm^2]	B_3 [μm^2]
As_2S_3 [26]	1.898	1.922	0.876	0.0225	0.0625	0.1225

The dispersion of the fiber includes the waveguide and the material dispersion. It is determined by equation (2) [27]:

$$D(\lambda) = -\frac{\lambda}{c} \frac{d^2 \text{Re}[n_{eff}]}{d\lambda^2} \quad (2)$$

where $\text{Re}[n_{eff}]$ stands for the real part of the effective refractive index obtained from the simulation and c is the speed of light in a vacuum. When light travels in a photonic crystal fiber, the effective refractive index is determined by formula (3):

$$n_{eff} = \frac{\beta_{pm}}{k_0} \quad (3)$$

here, $k_{zpm} = \beta_{pm}$, p is the polarization (TE or TM), m is the m^{th} mode of polarization, k_0 is the number of waves in free space for a given frequency of light and is defined $k_0 = \frac{\omega}{c} = \frac{2\pi\nu}{c} = \frac{2\pi}{\lambda_0}$, λ_0 is the wavelength in free space, ν is the frequency of all media.

III. RESULTS AND DISCUSSION

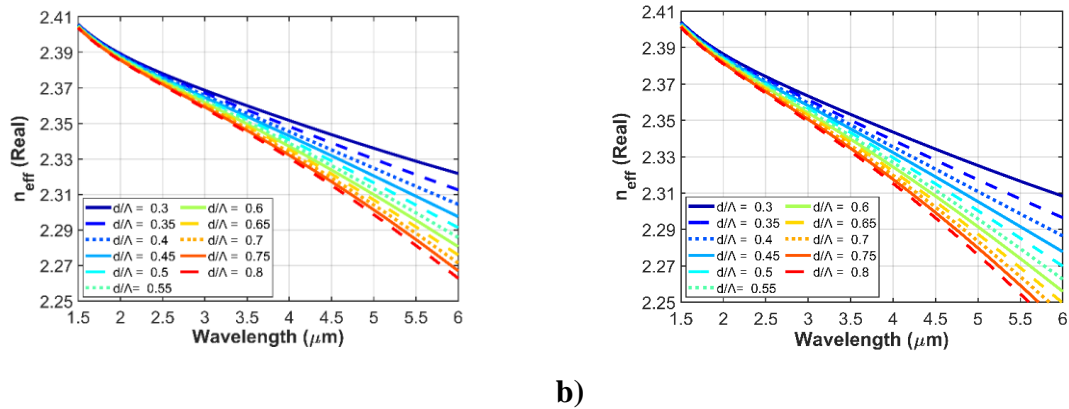


Fig. 2. The real part of effective refractive index as a function of wavelength with $\Lambda = 1.0 \mu\text{m}$, $d/\Lambda = 0.3 \div 0.8$ for two PCF structures: a) circular lattice; b) hexagonal lattice.

In Fig. 2, the effective refractive index (n_{eff}) of the elementary modes in the proposed PCFs is calculated for the structures whose fill factor varies from 0.3 to 0.8 with a lattice constant of $1.0 \mu\text{m}$. As seen in these graphs, the effective refractive index of circular and hexagonal PCFs changes with the change of wavelength, the filling factor d/Λ , and has a similar shape. It is noteworthy that as the wavelength increases, the effective refractive index decreases significantly. The reason is that longer wavelengths have a stronger ability to penetrate the PCF coverage area than shorter wavelengths [28]. Meanwhile, the effective refractive index of the circular lattice is always larger than that of the hexagonal lattice in the investigated wavelength range, and the effective refractive index decreases as the wavelength increases. It can be seen that the change of effective refractive index is mainly influenced by the filling factor parameter d/Λ . This result is exactly the same for both fiber structures.

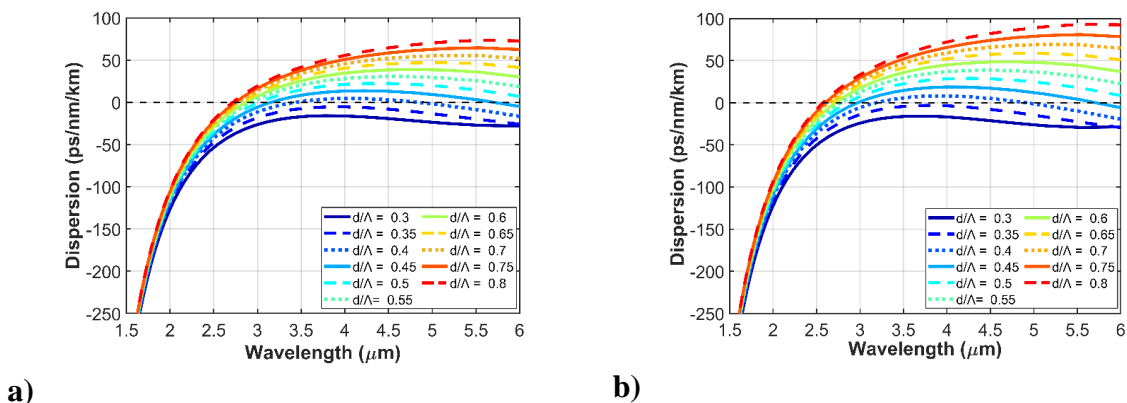


Fig. 3. Dispersion of PCF by wavelength with different d/Λ values gives $\Lambda = 1.0 \mu\text{m}$ for two structures: a) circular lattice; b) hexagonal lattice.

Fig. 3 shows how changing the fill factor (d/Λ) affects the dispersion (D). Looking at the histogram, we see that the two lattice structures have chromaticity varying with different wavelengths, the resulting chromatic curves include all-normal dispersion and anomalous dispersion with one or two zero-dispersion wavelengths. The dispersion characteristic is dominated by the change of the filling factor d/Λ . Furthermore, the change of this parameter causes the ZDW to switch to a longer wavelength. As observed, we see the dispersion lines in both types of lattice have similar shapes. Specifically, at lattice constant = $1.0 \mu\text{m}$ (Fig. 3), for both circular lattice (Fig. 3a) and hexagonal lattice (Fig. 3b), each type of lattice has two all-

normal dispersion curves that usually appear at $d/\Lambda = 0.3$ and $d/\Lambda = 0.35$. As the fill factor increases, anomalous dispersion curves begin to appear. An anomalous dispersion curve with a ZDW occurs when $d/\Lambda = 0.5 - 0.8$. Meanwhile, anomalous color curves with two ZDWs only appeared in two fibers with $d/\Lambda = 0.4 - 0.45$. It can be seen that the change of the filling factor (d/Λ) has made many dispersion characteristics of PCF appear.

Dispersion is one of the key factors for supercontinuum emission, the flat dispersion fiber allows for a wider SCG to be obtained. Therefore, fiber structures with flat dispersion curve and close to zero dispersion curve, and pump wavelength compatible ZDW has always been the goal of dispersion optimization. Based on preliminary simulations, we propose six fibers with optimal dispersion for the two types of lattice. In circular lattice structures, we select fibers with optimal dispersion for analysis as #F₁, #F₂, and #F₃, respectively. Meanwhile, #F₄, #F₅, and #F₆ are the selected hexagonal lattice structures, respectively. The structural parameters of the optimized fibers are shown in Table 2.

Table 2. Structural parameters of the proposed fibers.

Type	Fiber	d/Λ
Circular lattice	#F ₁	0.35
	#F ₂	0.5
	#F ₃	0.4
Hexagonal lattice	#F ₄	0.35
	#F ₅	0.5
	#F ₆	0.4

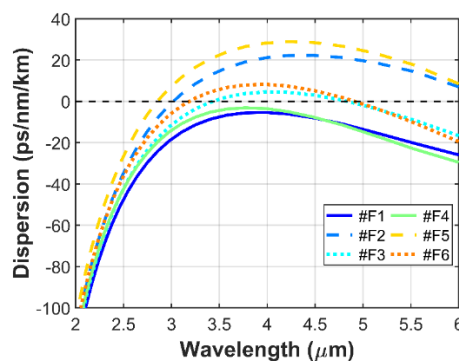


Fig. 4. Dispersion characteristics of the proposed fibers.

The dispersion characteristics of the proposed fibers #F₁, #F₂, #F₃, #F₄, #F₅ and #F₆ are shown in Fig. 4. It can be seen that the proposed fibers have flat dispersion, close to zero in the wide wavelength range, which is a decisive factor in the creation of ultra-wideband SC.

Table 3 shows the dispersion value at the pump wavelength of the proposed fibers. The all-normal dispersion curve #F₁ has a maximum dispersion value of $-5.7 \text{ ps} \cdot (\text{nm} \cdot \text{km})^{-1}$ at wavelength 3.98, so we choose a pump wavelength for fiber #F₁ to be 4.0 μm. Threads #F₃, #F₄ and #F₆ have the same pumping wavelength as #F₁ which is 4.0. While fibers #F₂ and #F₅ exhibit anomalous dispersion with a ZDW at wavelength 3.0 μm, the pump wavelength of this fiber is chosen to be 3.5 μm. Dispersion values of #F₂ and #F₅ fibers at pump wavelength 3.5 μm are $14.65 \text{ ps} \cdot (\text{nm} \cdot \text{km})^{-1}$ and $22.395 \text{ ps} \cdot (\text{nm} \cdot \text{km})^{-1}$, respectively. Meanwhile, the dispersion value at pump wavelength 4.0 μm of fibers #F₁, #F₃, #F₄ and #F₆ is $-5.53 \text{ ps} \cdot (\text{nm} \cdot \text{km})^{-1}$, $4.45 \text{ ps} \cdot (\text{nm} \cdot \text{km})^{-1}$, $-3.89 \text{ ps} \cdot (\text{nm} \cdot \text{km})^{-1}$ and $7.87 \text{ ps} \cdot (\text{nm} \cdot \text{km})^{-1}$, respectively.

Table 3. Dispersion value at pump wavelength of the proposed fibers.

#	Pump wavelength (μm)	D ($\text{ps} \cdot (\text{nm} \cdot \text{km})^{-1}$)
#F ₁	4.0	-5.53
#F ₂	5.5	14.65
#F ₃	4.0	4.45
#F ₄	4.0	-3.89
#F ₅	4.5	22.395
#F ₆	4.0	7.87

IV. CONCLUSION

In this paper, we have designed two novel solid-core photonic crystal fiber structures using As_2S_3 substrates consisting of six air-hole rings arranged in a circular and hexagonal lattice. We analyze the effective refractive index and dispersion characteristics of the two designed structures. Then compare the characteristics of the two types of structures. The two structures generally have similar effective refractive index and dispersion graphs. The PCF structures all acquire diverse dispersion properties including all-normal dispersion and anomalous dispersion with one or two zero dispersion wavelengths (ZDWs). On the basis of analysis and comparison, we have proposed a structure with optimal dispersion and suitable pumping wavelength for supercontinuum generation with a wide, flat, and smooth spectrum.

ACKNOWLEDGEMENT. This research is funded by Vietnam's Ministry of Education and Training (B2023-TDV-07). Dang Van Trong was funded by the Master, PhD Scholarship Programme of Vingroup Innovation Foundation (VINIF), code [VINIF.2022.TS136].

REFERENCES

- [1] J.C. Knight, T.A. Birks, P.S.J. Russell, D.M. Atkin, *Optics Letters*, **21**, 1996, pp. 1547-1549.
- [2] J.C. Knight, *Nature*, **424**, 2003, pp. 847-851.
- [3] L.C. Van, V.T. Hoang, V.C. Long, K. Borzycki, K.D. Xuan, V.T. Quoc, M. Trippenbach, R. Buczyński and J.Pniewski, *Laser Phys.*, **30**, 2020, pp. 035105.
- [4] L.C. Van, V.T. Hoang, V.C. Long, K. Borzycki, K.D. Xuan, V.T. Quoc, M. Trippenbach, R.Buczyński, and J.Pniewski, *Laser Phys.*, **29**, 2019, pp. 075107.
- [5] K.D. Xuan, L.C. Van, Q.H. Dinh, L.V. Xuan, M. Trippenbach, and R. Buczynski, *Applied Optics*, **56**, 2017, pp. 1012-1019.
- [6] K.D. Xuan, L.C. Van, V.C. Long, Q.H. Dinh, L.V. Mai, M. Trippenbach, and R. Buczyński, *Optical and Quantum Electronics*, **49**, 2017, pp. 87.
- [7] H.Q. Quy and L.C. Van, *Indian Journal of Pure & Applied Physics*, **59**, 2021, pp. 522-527.
- [8] A. Medjouri, A.M. Simohamed, O. Ziane, and A. Boudrioua, *Optik- International Journal for Light and Electron Optics*, **126**, 2015, pp. 5718-5724.

The 8th Academic Conference On Natural Science For Young Scientists, Master And Ph.D Students From Asean Countries, 28-30 August 2023, Vinh City, Vietnam

- [9] S.K. Pandey, Y.K. Prajapati, and J.B. Maur, *Results in Optics*, **1**, 2020, pp. 100024
- [10] S. Sen, Md. Abdullah-Al-Shafi, and M.A. Kabir, *Sensing and Bio-Sensing Research*, **30**, 2020, pp. 100377.
- [11] Y.E. Monfared, A.R.M. Maleki Javan, and A.R.M. Kashani, *Optik- International Journal for Light and Electron Optics*, **124**, 2013, pp. 7049-7052
- [12] Y. Wang, S. Li, J. Wu, P. Yu, and Z. Li, *Photonics and Nanostructures - Fundamentals and Applications*, **41**, 2020, pp. 100816.
- [13] C.V. Lanh, N.Q. Vu, N.T.M. Linh, T.Q. Vu, C.T.G. Trang, D.T. Huyen Dinh, N.T. Thuy, and D.X. Khoa, *Advances in Applied and Engineering Physics – CAEP VI*, 2020, pp. 288-291
- [14] D.V. Trong, L.T.B. Tran, V.T.M. Ngoc, T.D. Tan, C.V. Lanh, H.T. Duc, and N.T. Thuy, *The 7th Academic Conference on Natural Science for Young Scientists, Master and Ph.D. Students from ASEAN Countries (CASEAN – 7)*., 14-17, October 2021, pp. 293-300.
- [15] N.T. Thuy, H.T. Duc, D.V. Trong, L.T.B. Tran, D.V. Hung, and C.V. Lanh, *The 7th Academic Conference on Natural Science for Young Scientists, Master and Ph.D. Students from ASEAN Countries*, 14-17, October 2021, pp. 309-316.
- [16] C. Vigreux-Bercovici, V. Ranieri, L. Labadie, J.E. Broquin, P. Kern, and A. Pradel, *Journal of Non-Crystalline Solids*, **352**, 2006, pp. 23-25.
- [17] N.T. Thuy, H.T. Duc, D.V. Trong, L.T.B. Tran, and C.V. Lanh, *Hue University Journal of Science: Natural Science*, **130**, 2021, pp. 55-64.
- [18] A. S. J. Choyon and R. Chowdhury, *Optik*, **258**, 2020, pp. 168857.
- [19] K. F. Fiaboe, S. Singh, R. Rai, and P. Kumar, *J. Emerging Tech. Innovative Research*, **6**, 2019, pp. 280-285.
- [20] A. S. J. Choyon and R. Chowdhury, *Optik*, **258**, 2022, 168857 (11pp).
- [21] N. Wang, J. L. Xie, H. Z. Jia, and M. M. Chen, *J. Modern Opt.*, **65**, 2018, pp. 2060-2064.
- [22] T. Peng, T. Xu, and X. Wang, *IEEE Access*, **5**, 2017, pp. 17240-17245.
- [23] M. Asobe, T. Kanamori, and K. Kubodera, *IEEE Photonics Technology Letters*, **4**, 1992, pp. 362-365.
- [24] <https://www.lumerical.com/products/mode>
- [25] S. Kedenburg, M. Vieweg, T. Gissibl, and H. Giessen, *Optical Materials Express*, **2**, 2012, pp. 1588-1611.
- [26] W.S. Rodney, I.H. Malitson, and T.A. King, *Journal of the Optical Society of America*, **48**, 1958, pp. 633-635.
- [27] R. Buczyński, *Acta Phys. Pol. A.*, **106**, 2004, pp. 141-168.
- [28] P. Dhara and V.K. Singh, *Microsystem Technologies.*, **27**, 2021, pp. 127-132.